

Binary Population and Spectral Synthesis (BPASS)

Version 2.2: Tuatara
(subversion 2.2.1)

User Manual

The Binary Population and Spectral Synthesis (BPASS) models are a set of stellar evolution and spectral synthesis models that can be used to model a broad range of stellar populations and their properties. This manual gives an overview of the models and the contents of the BPASS v2.2 data release.

See also:

Stanway & Eldridge (2018, MNRAS in press) for v2.2 release

Eldridge, Stanway et al (2017, PASA, 34, 58) for v2.1 details

Table of Contents

| | |
|--|-----------|
| 1 - Introduction | 4 |
| 2 - BPASS Acknowledgement | 5 |
| 3 - Outline of BPASS Models and Methods | 6 |
| 4 - Caveats and Cautions | 11 |
| 5 - Data Release | 12 |
| README: Spectral Energy Distributions | 13 |
| README: Supernova Rate Files | 14 |
| README: Stellar Type Numbers | 14 |
| README: Yields | 15 |
| README: Surviving Stellar Masses | 16 |
| README: Ionizing Photon Rates | 16 |
| README: Colours | 16 |
| README: Lick Indices | 17 |
| README: Mass-to-Light Ratios | 18 |
| README: Hertzsprung-Russell diagram isocontours | 18 |
| README: Inputs | 20 |
| README: Stellar Models | 20 |
| README: O Star Atmosphere Models | 23 |
| 6 - Post-Processed Data Products | 24 |
| CLOUDY and Nebular gas | 24 |
| Dust Absorption and Re-emission | 25 |
| Complex Star Formation Histories | 26 |
| 7 - Recent Key Results and Calibration Tables | 28 |
| Z-dependent Star Formation Rate Conversion Factors for $H\alpha$ and FUV | 28 |
| Maximal relations for BPASS binary starbursts in the BPT diagrams. | 29 |
| Rest-Ultraviolet Properties of Ongoing Starbursts (N_{ion} , L_{1500} , ξ_{ion}) | 30 |
| Z-dependent SN Rates for Constant SFR | 31 |
| 8 - Auxilliary Software | 32 |
| CMD plotting code - plot1cmdmake.pro and plot1cmdplot.pro | 32 |
| Example plotting codes | 33 |
| 9 - Areas under Development | 34 |
| 10 - The BPASS Team | 35 |
| Thanks | 36 |

1 - Introduction

The Binary Population and Spectral Synthesis (BPASS) suite of binary stellar evolution models and synthetic stellar populations provides a framework for the physically motivated analysis of both the integrated light from distant stellar populations and the detailed properties of those nearby. We present a new version 2.2 data release.

The BPASS code was initially established explicitly to explore the effects of massive star duplicity on the observed spectra arising from young stellar populations, both at Solar and sub-Solar metallicities (Eldridge & Stanway, 2009). In particular it was initially focused on interpreting the spectra of high redshift galaxies, in which stellar population ages of $< 100\text{Myr}$ and metallicities a few tenths of Solar dominate the observed properties (Eldridge & Stanway, 2012). It has since been expanded to confront a much broader range of environments and incorporate significantly more complete stellar populations.

We have also endeavored to make the results of the code easily available to all astronomers and astrophysicists who wish to use them. Our philosophy is to present these models on a ‘best-effort’ basis. We do not attempt to fine tune the models but use the best estimates we have to create the single star and binary populations. The model and parameters will only be updated or varied between future versions. We also make clear the caveats and limitations associated with the models. We do not claim infallibility, and would welcome suggestions for improvement, while noting that we cannot promise a rapid response to requests.

The term BPASS can be used interchangeably to refer to the stellar evolution code, the spectral population synthesis code, the resulting models or the collaborative project exploring and exploiting these models. For additional information or ‘on request’ outputs, please contact us at j.eldridge@auckland.ac.nz and e.r.stanway@warwick.ac.uk.

Key BPASS papers include:

- Eldridge J. J., Stanway E. R., 2009, MNRAS, 400, 1019
- Eldridge J. J., Stanway E. R., 2012, MNRAS, 419, 479
- Stanway E. R., Eldridge J. J., Becker G. D., 2016, MNRAS, 456, 485
- Eldridge, Stanway et al, 2017, PASA, 34, 58. (E+17)
- Stanway & Eldridge, 2018, MNRAS in press.

Additional papers providing input to BPASS or exploring applications include:

- Eldridge J. J., Izzard R. G., Tout C. A., 2008, MNRAS, 384, 1109
- Stanway E. R., Eldridge J. J., et al., 2014, MNRAS, 444, 3466
- Xiao L., Eldridge J. J., 2015, MNRAS, 452, 2597
- McClelland L. A. S., Eldridge J. J., 2016, MNRAS, 459, 1505
- Eldridge J. J., Stanway E. R., 2016, MNRAS, 462, 3302
- Xiao, Eldridge & Stanway, 2018, MNRAS, 477, 904.

2 - BPASS Acknowledgement

Modifications for BPASS v2.2 are described in Stanway & Eldridge (2018, MNRAS in press). This builds on extensive work described in detail in Eldridge, Stanway et al (2017, PASA, 34, 58), which also presents a range of validation tests. A copy of both papers (and this manual) can also be found in the README subdirectory of the data release.

Subversion v2.2.1 represents a minor fix in the scaling of one set of WD stellar spectra which makes <1% difference to virtually all outputs but led to negative fluxes at a handful of ages and wavelengths.

We would appreciate the inclusion of the following acknowledgement where appropriate:
“This work made use of v2.2.1 of the Binary Population and Spectral Synthesis (BPASS) models as last described in Stanway & Eldridge (2018).”

3 - Outline of BPASS Models and Methods

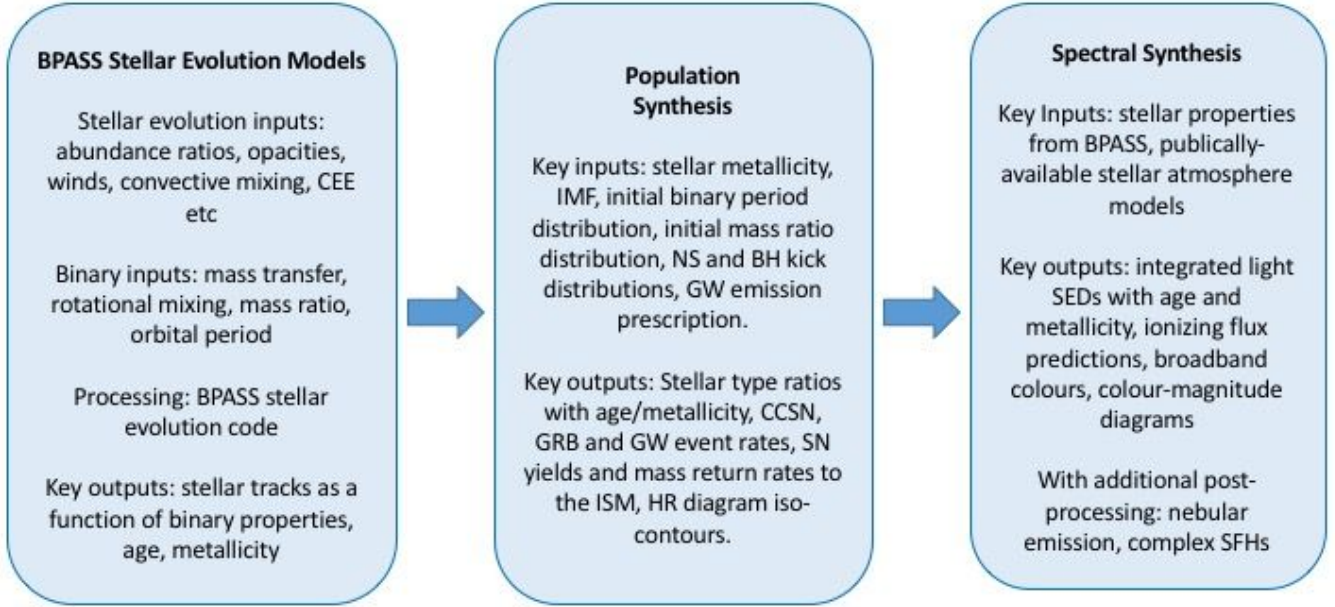
BPASS is based on a custom stellar evolution model code, first discussed in Eldridge et al. (2008), which was originally based in turn on the long-established Cambridge STARS stellar evolution code (Eggleton, 1971; Pols et al., 1995; Eldridge & Tout, 2004b). The structure, temperature and luminosity of both individual stars and interacting binaries are followed through their evolutionary history, carefully accounting for the effects of mass and angular momentum transfer. The original BPASS prescription for spectral synthesis of stellar populations from individual stellar models was described in Eldridge & Stanway (2009, 2012), while a study of the effect of supernova kicks on runaway stars and supernova populations was described in Eldridge et al. (2011). In the years since this initial work, a large number of additions and modifications have been made to the BPASS model set, resulting in a version 2.0 data release in 2015 which is briefly detailed in Stanway et al. (2016) and Eldridge & Stanway (2016). It has been widely used by the stellar (e.g. Blagorodnova et al., 2017; Wofford et al., 2016) and extragalactic (e.g. Ma et al., 2016; Steidel et al., 2016) communities but was not formally described until the v2.1 (Kiwi) data release paper of Eldridge, Stanway et al (2017, hereafter E+17). This is the most thorough description of the BPASS pipeline and procedure and remains the fundamental reference for the details of the model. The v2.2 data release (Tuatara) is focussed on improved treatment of stellar populations at ages > 1 Gyr. Subversion v2.2.1 represents a minor fix in the scaling of one set of WD stellar spectra which makes $< 1\%$ difference to virtually all outputs but led to negative fluxes at a handful of wavelengths.

From version 2.1 (Kiwi) onwards, BPASS models are associated with version names. Version 2.2, with its focus on old stellar populations, is named “Tuatara” after the New Zealand-native reptile which has been identified as a living fossil and which retains characteristics of its origin as a species ~ 220 Myr ago.

The more important new features included in this release of BPASS include: a change in our input binary parameter distributions, calculation of a significantly larger number of stellar models, a change in our default main-sequence stellar atmosphere models, two additional initial mass functions, and a revision of our rejuvenation and AGB branch prescriptions. Lick indices and stellar mass-to-light ratios have been added to the outputs.

Some of the input terms (e.g. relative elemental abundance ratios, opacities, mixing, mass transfer prescriptions, kicks etc) are fixed in the stellar evolution code and discussed in the v2.1 data release paper. All models use a fixed, abundance ratio prescription based on solar abundances.

Generation of the BPASS models can be broadly divided into three main stages, each with associated outputs:



The seven IMFs calculated as part of our model set are defined by broken power laws as follows:

$$N(M < M_{\max}) \propto \int_{0.1}^{M_1} \left(\frac{M}{M_{\odot}} \right)^{\alpha_1} dM + M_1^{\alpha_1} \int_{M_1}^{M_{\max}} \left(\frac{M}{M_{\odot}} \right)^{\alpha_2} dM$$

(see table 1, Stanway & Eldridge 2018)

| Model | α_1 (0.1 M_{\odot} - M_1) | α_2 (M_1 - M_{\max}) | M_1 | M_{\max} |
|------------|--|--------------------------------------|-------|-----------------|
| 100_100 | -1.30 | -2.00 | 0.5 | 100 M_{\odot} |
| 100_300 | -1.30 | -2.00 | 0.5 | 300 M_{\odot} |
| 135_100 | -1.30 | -2.35 | 0.5 | 100 M_{\odot} |
| 135_300 | -1.30 | -2.35 | 0.5 | 300 M_{\odot} |
| 135all_100 | -2.35 | -2.35 | 0.5 | 100 M_{\odot} |
| 170_100 | -1.30 | -2.70 | 0.5 | 100 M_{\odot} |
| 170_300 | -1.30 | -2.70 | 0.5 | 300 M_{\odot} |
| chab100 | exp cutoff | -2.3 | 1.0 | 100 M_{\odot} |
| chab300 | exp cutoff | -2.3 | 1.0 | 300 M_{\odot} |

Table 1. The range of stellar initial mass functions (IMFs) calculated in BPASS v2.2. Our default IMF is “135_300” and results in this paper are calculated using that IMF unless stated otherwise. “exp cutoff” indicates an exponential cut-off in the mass distribution following the prescription of [Chabrier \(2003\)](#).

Broken power law IMFs are labelled “imfxxx_yyy” where “xxx” is given by the upper slope and yyy by the upper limit on the stellar mass. Our default is imf135_300 and results in E+17 and later papers are based on this unless otherwise specified. The Salpeter (1955) IMF is reproduced by IMF number 5. It is labelled with “imf135all_100”

In v2.2 we also introduce two IMFs which follow the prescription of Chabrier (2003) for the gradual turn over and cut-off of the stellar mass distribution below 1 Msun. These are “imf_chab100” and “imf_chab300” where the number indicates an upper mass limit.

The key parameters considered in the model set are given in the following table:

Table 1: BPASS v2.2 input parameter ranges

| Parameter | Permitted Values |
|----------------------------|---|
| Single Star Models | $M_S = 0.1, 0.12, 0.14, 0.16, 0.18, 0.2, 0.22, 0.24, 0.26, 0.28, 0.3, 0.32, 0.34, 0.36, 0.38, 0.4, 0.42, 0.44, 0.46, 0.48, 0.5, 0.52, 0.54, 0.56, 0.58, 0.6, 0.62, 0.64, 0.66, 0.68, 0.7, 0.72, 0.74, 0.76, 0.78, 0.8, 0.82, 0.84, 0.86, 0.88, 0.9, 0.92, 0.94, 0.96, 0.98, 1, 1.02, 1.04, 1.06, 1.08, 1.1, 1.12, 1.14, 1.16, 1.18, 1.2, 1.22, 1.24, 1.26, 1.28, 1.3, 1.32, 1.34, 1.36, 1.38, 1.4, 1.42, 1.44, 1.46, 1.48, 1.5, 1.52, 1.54, 1.56, 1.58, 1.6, 1.62, 1.64, 1.66, 1.68, 1.7, 1.72, 1.74, 1.76, 1.78, 1.8, 1.82, 1.84, 1.86, 1.88, 1.9, 1.92, 1.94, 1.96, 1.98, 2, 2.05, 2.1, 2.15, 2.2, 2.25, 2.3, 2.35, 2.4, 2.45, 2.5, 2.55, 2.6, 2.65, 2.7, 2.75, 2.8, 2.85, 2.9, 2.95, 3, 3.1, 3.2, 3.3, 3.4, 3.5, 3.6, 3.7, 3.8, 3.9, 4, 4.1, 4.2, 4.3, 4.4, 4.5, 4.6, 4.7, 4.8, 4.9, 5, 5.1, 5.2, 5.3, 5.4, 5.5, 5.6, 5.7, 5.8, 5.9, 6, 6.1, 6.2, 6.3, 6.4, 6.5, 6.6, 6.7, 6.8, 6.9, 7, 7.1, 7.2, 7.3, 7.4, 7.5, 7.6, 7.7, 7.8, 7.9, 8, 8.1, 8.2, 8.3, 8.4, 8.5, 8.6, 8.7, 8.8, 8.9, 9, 9.1, 9.2, 9.3, 9.4, 9.5, 9.6, 9.7, 9.8, 9.9, 10, 11, 12, 13, 14, 15, 16, 17, 18, 19, 20, 21, 22, 23, 24, 25, 26, 27, 28, 29, 30, 31, 32, 33, 34, 35, 36, 37, 38, 39, 40, 41, 42, 43, 44, 45, 46, 47, 48, 49, 50, 51, 52, 53, 54, 55, 56, 57, 58, 59, 60, 61, 62, 63, 64, 65, 66, 67, 68, 69, 70, 71, 72, 73, 74, 75, 76, 77, 78, 79, 80, 81, 82, 83, 84, 85, 86, 87, 88, 89, 90, 91, 92, 93, 94, 95, 96, 97, 98, 99, 100, 125, 150, 175, 200, 225, 250, 275, 300 M_{\odot}.$ |
| Primary Model Masses | $M_1 = 0.1, 0.2, 0.3, 0.4, 0.5, 0.6, 0.8, 0.9, 1, 1.1, 1.2, 1.3, 1.4, 1.5, 1.6, 1.7, 1.8, 1.9, 2, 2.1, 2.3, 2.5, 2.7, 3, 3.2, 3.5, 3.7, 4, 4.5, 5, 5.5, 6, 6.5, 7, 7.5, 8, 8.5, 9, 9.5, 10, 11, 12, 13, 14, 15, 16, 17, 18, 19, 20, 21, 22, 23, 24, 25, 30, 35, 40, 50, 60, 70, 80, 100, 120, 150, 200, 300 M_{\odot}$. |
| Primary Model Mass Ratios | $M_2/M_1 = 0.1, 0.2, 0.3, 0.4, 0.5, 0.6, 0.7, 0.8, 0.9$ |
| Secondary Model Masses | $M_2 = 0.1, 0.2, 0.3, 0.4, 0.5, 0.6, 0.8, 0.9, 1.0, 1.1, 1.2, 1.3, 1.4, 1.5, 1.6, 1.7, 1.8, 1.9, 2, 2.1, 2.3, 2.5, 2.7, 3, 3.2, 3.5, 3.7, 4, 4.5, 5, 5.5, 6, 6.5, 7, 7.5, 8, 8.5, 9, 9.5, 10, 11, 12, 13, 14, 15, 16, 17, 18, 19, 20, 21, 22, 23, 24, 25, 30, 35, 40, 50, 60, 70, 80, 100, 120, 150, 200, 300, 400$ and $500 M_{\odot}$. |
| Compact remnant masses | $\log(M_{\text{rem},1}/M_{\odot}) = -1, -0.9, -0.8, -0.7, -0.6, -0.5, -0.4, -0.3, -0.2, -0.1, 0, 0.1, 0.2, 0.3, 0.4, 0.5, 0.6, 0.7, 0.8, 0.9, 1, 1.1, 1.2, 1.3, 1.4, 1.5, 1.6, 1.7, 1.8, 1.9$ and 2 . |
| Binary Period | 21 initial periods from $\log(P/\text{days}) = 0, 0.2, 0.4, 0.6, 0.8, 1, 1.2, 1.4, 1.6, 1.8, 2, 2.2, 2.4, 2.6, 2.8, 3, 3.2, 3.4, 3.6, 3.8, 4.0$ |
| Binary Parameters | Binary parameter distribution described by table 13 of Moe & Di Stefano (2017) |
| Stellar Ages | Output ages from $\log(\text{Age}/\text{yrs}) = 6.0$ to 11.0 (1 Myr to 100 Gyr) |
| Metallicity Mass Fractions | $Z = 10^{-5}, 10^{-4}, 0.001, 0.002, 0.003, 0.004, 0.005, 0.006, 0.008, 0.010, 0.014, 0.020 (Z_{\odot}), 0.030, 0.040$ |
| Initial Mass Functions | 9 different mass functions - fiducial version: has an IMF slope of -1.30 from 0.1 to $0.5 M_{\odot}$, and a slope of -2.35 from 0.5 to $300 M_{\odot}$. |
| Stellar Atmospheres | CKC14 ($\log g = -1$ to 5.5 , $(T/K) = 2500$ to 25000 and $\log(Z/Z_{\odot}) = -3$ to 0.5). BASEL v2.2 ($\log g = -1$ to 5.5 , $(T/K) = 2000$ to 50000 and $\log(Z/Z_{\odot}) = -3.5$). PoWR (We use the SMC and LMC, WN grids with $X_{\text{surface}} = 0.4, 0.2$ and 0 . For the Galaxy we use the WN grids with $X_{\text{surface}} = 0.5, 0.2$ and 0 . At all metallicities we use the Galactic WC grid.) WMBASIC (v2.1 model grid for O stars, described in E+17). Levenhagan et al (2017, DA WDs, $\log g = 7.0$ to 9.5 , $(T/K) = 17000$ to $100,000$). |

For the binary population synthesis, we now assume a distribution of binary parameters as given in table 13 of Moe & Di Stefano (2017, reproduced on the next page for reference). In brief, this provides the binary fraction and initial period distribution as a function of primary star mass. It also provides a broken power law distribution for the binary mass ratio as a function of mass and initial period, and a ‘twin’ fraction which is used to supplement the highest mass ratio bin ($M1/M2=0.9$) in our model set.

These parameter distributions are used in combination with the initial mass function to determine the initial weighting of the single star and primary star models in our population synthesis. Secondary models, chemically homogenous evolution models and additional single star models are then added during population synthesis to represent systems in which the primary has reached the end of its evolution, post-mass transfer low metallicity systems, and post-merger or disrupted binary systems respectively.

We note that the Moe & Di Stefano meta-analysis was based on local stellar populations. While we use the same distributions at much lower metallicity, there is currently no way to verify the dependence of binary parameter distributions in such a situation. In the event that a lower binary fraction is required, we also provide single star populations that can be mixed in proportion to reduce the overall binary fraction. We caution that we do not recommend using our single star models in isolation.

Table 13
Multiplicity Statistics as a Function of Primary Mass/Spectral Type after Correcting for Observational Selection Effects

| Statistic | Explanation | Solar-type $M_1 = 0.8\text{--}1.2 M_\odot$ | A/late B $M_1 = 2\text{--}5 M_\odot$ | Mid-B $M_1 = 5\text{--}9 M_\odot$ | Early B $M_1 = 9\text{--}16 M_\odot$ | O-type $M_1 > 16 M_\odot$ |
|---|-----------------------------------|---|---|--------------------------------------|---|------------------------------|
| $f_{\text{mult}; q > 0.1}$ | Total multiplicity frequency | 0.50 ± 0.04 | 0.84 ± 0.11 | 1.3 ± 0.2 | 1.6 ± 0.2 | 2.1 ± 0.3 |
| $f_{\log P < 3.7; q > 0.1}$ | Close binary frequency | 0.15 ± 0.03 | 0.37 ± 0.08 | 0.63 ± 0.13 | 0.8 ± 0.2 | 1.0 ± 0.2 |
| $\mathcal{F}_{n=0; q > 0.1}$ | Single-star fraction | 0.60 ± 0.04 | 0.41 ± 0.08 | 0.24 ± 0.08 | 0.16 ± 0.09 | 0.06 ± 0.06 |
| $\mathcal{F}_{n=1; q > 0.1}$ | Binary-star fraction | 0.30 ± 0.04 | 0.37 ± 0.06 | 0.36 ± 0.08 | 0.32 ± 0.10 | 0.21 ± 0.11 |
| $\mathcal{F}_{n \geq 2; q > 0.1}$ | Triple- + quadruple-star fraction | 0.10 ± 0.02 | 0.22 ± 0.07 | 0.40 ± 0.10 | 0.52 ± 0.13 | 0.73 ± 0.16 |
| Companion frequency across: | | | | | | |
| $f_{\log P=1; q > 0.1}$ | $\log P = 0.5\text{--}1.5$ | 0.027 ± 0.009 | 0.07 ± 0.02 | 0.14 ± 0.04 | 0.19 ± 0.06 | 0.29 ± 0.08 |
| $f_{\log P=3; q > 0.1}$ | $\log P = 2.5\text{--}3.5$ | 0.057 ± 0.016 | 0.12 ± 0.04 | 0.22 ± 0.07 | 0.26 ± 0.09 | 0.32 ± 0.11 |
| $f_{\log P=5; q > 0.1}$ | $\log P = 4.5\text{--}5.5$ | 0.095 ± 0.018 | 0.13 ± 0.03 | 0.20 ± 0.06 | 0.23 ± 0.07 | 0.30 ± 0.09 |
| $f_{\log P=7; q > 0.1}$ | $\log P = 6.5\text{--}7.5$ | 0.075 ± 0.015 | 0.09 ± 0.02 | 0.11 ± 0.03 | 0.13 ± 0.04 | 0.18 ± 0.05 |
| Excess twin fraction at: | | | | | | |
| $\mathcal{F}_{\text{twin}}$ | $\log P = 1$ | 0.30 ± 0.09 | 0.22 ± 0.07 | 0.17 ± 0.05 | 0.14 ± 0.04 | 0.08 ± 0.03 |
| $\mathcal{F}_{\text{twin}}$ | $\log P = 3$ | 0.20 ± 0.06 | 0.10 ± 0.04 | <0.03 | <0.03 | <0.03 |
| $\mathcal{F}_{\text{twin}}$ | $\log P = 5$ | 0.10 ± 0.03 | <0.03 | <0.03 | <0.03 | <0.03 |
| $\mathcal{F}_{\text{twin}}$ | $\log P = 7$ | <0.03 | <0.03 | <0.03 | <0.03 | <0.03 |
| Power-law slope of $p_q \propto q^\gamma$ across $q = 0.3\text{--}1.0$ at: | | | | | | |
| $\gamma_{\text{large}q}$ | $\log P = 1$ | -0.5 ± 0.3 | -0.5 ± 0.3 | -0.5 ± 0.3 | -0.5 ± 0.3 | -0.5 ± 0.3 |
| $\gamma_{\text{large}q}$ | $\log P = 3$ | -0.5 ± 0.3 | -0.9 ± 0.3 | -1.7 ± 0.3 | -1.7 ± 0.3 | -1.7 ± 0.3 |
| $\gamma_{\text{large}q}$ | $\log P = 5$ | -0.5 ± 0.3 | -1.4 ± 0.3 | -2.0 ± 0.3 | -2.0 ± 0.3 | -2.0 ± 0.3 |
| $\gamma_{\text{large}q}$ | $\log P = 7$ | -1.1 ± 0.3 | -2.0 ± 0.3 | -2.0 ± 0.3 | -2.0 ± 0.3 | -2.0 ± 0.3 |
| Power-law slope of $p_q \propto q^\gamma$ across $q = 0.1\text{--}0.3$ at: | | | | | | |
| $\gamma_{\text{small}q}$ | $\log P = 1$ | 0.3 ± 0.4 | 0.2 ± 0.4 | 0.1 ± 0.4 | 0.1 ± 0.4 | 0.1 ± 0.4 |
| $\gamma_{\text{small}q}$ | $\log P = 3$ | 0.3 ± 0.6 | 0.1 ± 0.6 | -0.2 ± 0.6 | -0.2 ± 0.6 | -0.2 ± 0.6 |
| $\gamma_{\text{small}q}$ | $\log P = 5$ | 0.3 ± 0.4 | -0.5 ± 0.4 | -1.2 ± 0.4 | -1.2 ± 0.4 | -1.2 ± 0.4 |
| $\gamma_{\text{small}q}$ | $\log P = 7$ | 0.3 ± 0.3 | -1.0 ± 0.3 | -1.5 ± 0.3 | -1.5 ± 0.3 | -1.5 ± 0.3 |

Moe & Di Stefano, 2017, ApJS, 230, 15 - Table 13

4 - Caveats and Cautions

Caveats and cautions regarding the use of BPASS v2.2 are discussed in Stanway & Eldridge (2018) and a more extensive list of fundamental issues is given in E+17.

In brief, uncertainties within our models continue to affect the following areas:

Type Ia supernova rates - while these are substantially improved in v2.2, we note that they are currently unverified and are still subject to uncertainties discussed below.

Rotational mixing - both in isolated stars and as a result of spin up by mass transfer.

Common envelope evolution - we use a relatively simple CEE prescription which may substantially impact the production of compact remnants (WDs, NSs).

Composition - studies of individual spectral features may be affected by varying abundance ratios (e.g. α -enhancement).

Wolf-Rayet star inflation - an improved prescription may lower stellar temperatures.

Neutron star and binary kicks - the distribution of kick velocities will have implications for type Ia SNe and compact object merger GW event rates.

We also caution that BPASS is concerned solely with the *stellar* component in systems, and generates simple (i.e. single-aged) stellar populations (SSPs). Treatment of nebular gas, dust or non-thermal components, or of complex star formation histories, in comparison to observed sources requires post-processing of the data release products.

5 - Data Release

The BPASS v2.2 data release comprises the following primary data products:

1. Stellar Model Outputs:

- (a) Binary stellar models with photometric colours
- (b) OB stellar atmospheres (unchanged since v2.1)

2. Stellar Population Outputs (all versus age):

- (a) Massive star type number counts
- (b) Core collapse supernova rates
- (c) Yields, energy output from winds and supernovae and ejected yields of X , Y and Z
- (d) Stellar population mass remaining
- (e) HR diagram (isochronal contours)

3. Spectral Synthesis Outputs (all versus age):

- (a) Spectral Energy Distributions
- (b) Ionizing flux predictions
- (c) Broadband colours
- (d) Colour-Magnitude Diagram (CMD) making code
- (e) Lick indices and mass-to-light ratios

4. Available on request due to unverified status:

- (a) Approximate accretion luminosities from X- ray binaries
- (b) A limited set of nebula emission models (still based on v2.1, not v2.2)

All outputs of the current BPASS v2.1 data release can be found at <http://bpass.auckland.ac.nz>, and are mirrored at <http://warwick.ac.uk/bpass>.

For additional information or ‘on request’ outputs, please contact us at j.eldridge@auckland.ac.nz and e.r.stanway@warwick.ac.uk

Each file gives results for a simple stellar population (i.e. instantaneous starburst) which initially formed 10^6 Msun of stars, at ages from $\log(\text{age}/\text{years})=6.0$ to $\log(\text{age}/\text{years})=11$ in 0.1 dex increments. The length of each time bin can be calculated as

$$\text{dt} = 10^{(\log(\text{age})+0.05)} - 10^{(\log(\text{age})-0.05)} \text{ years,}$$

except for the first bin which is $10^{6.05}$ years. We do not provide complex star formation histories, but these can be straightforwardly constructed (see *Post-Processed Data Products* below).

In each case the files are written to disk with a format “(n(E16.7))” where n is the number of columns, unless otherwise specified.

Values given as logarithms are in base 10, unless otherwise specified.

In most cases, a data file is provided for model outputs as a function of age at each metallicity, and separately for single and binary populations.

File names have been modified in this version release to remove any possibility of confusion. Each file name now incorporates both the model type (<opt> = ‘sin’ or ‘bin’) and the IMF label as defined on page 7 well as the metallicity.

<z> in file names denotes stellar metallicity mass fraction and can be “zem5”, “zem4”, “z001”, “z002”, “z003”, “z004”, “z006”, “z008”, “z010”, “z020”, “z030” or “z040”, where “zem5” implies $Z=1.0E-5$ and “z020” implies $Z = 0.020$ etc.

Where results are scaled by Solar metallicity, we assume $Z_{\text{sun}}=0.020$.

Where results are given in Solar luminosities, we assume $L_{\text{sun}}=3.848 \times 10^{26}$ J/s.

In the following pages, we provide README files for each data product.

README: Spectral Energy Distributions

These files contain the primary output of BPASS, which is the stellar spectral energy distribution (SED). Flux values are given every 1 Angstrom in the range 1 - 100,000 Å. Most users will wish to resample to lower resolution, depending on their use case. We caution that some of the stellar atmospheres we use also have slightly lower spectral resolution.

Each file has 52 columns and 10^6 rows. The first column lists a wavelength in angstroms, and each remaining column n ($n>1$) holds the model flux for the population at an age of $10^{(6+0.1*(n-2))}$ years at that wavelength.

The units of flux are Solar Luminosities per Angstrom, normalised for a cluster of $1e6$ M_{sun} formed in a single instantaneous burst. The total luminosity of the SED can be simply calculated by summing all the rows together. Or the flux over the wavelength

range from, for example, 2000 to 3000 Angstroms can be calculated by summing the 2000th to 3000th rows.

Filenames: spectra-<opt>-<imf>.<z>.dat

README: Supernova Rate Files

These files contain information regarding supernova rates. The numbers in the columns give the number of supernovae in each time bin, arising from a 10^6 Msun instantaneous burst of stars at $t=0$. For use when converting these numbers to rates we include the width of each time bin in the final column.

The estimated GRB rate is isotropic (i.e. not corrected for beaming angle) and assumes only pathways involving spin up by mass accretion and rotationally-mixed, chemically homogenous evolution (see E+17 for details). Other pathways may not be accounted for.

Where no number is provided, these events are sufficiently rare not to be represented in our standard synthesis models. Since these estimates are based on a finite number of stellar models we also include estimates of the uncertainty in the number of each supernova type in the later columns.

Column1 - $\log(\text{age}/\text{yrs})$

Column 2 - number of type Ia supernovae in bin

Column 3 - number of type IIP supernovae

Column 4 - number of type II-other supernovae

Column 5 - number of type Ib supernovae

Column 6 - number of type Ic supernovae

Column 7 - number of long-GRB supernovae - jet angle not accounted for

Column 8 - number of pair-instability supernovae

Column 9 - number of low-mass supernovae (final mass $<2M_{\text{sun}}$).

Columns 10-17 poisson errors for above supernova numbers

Columns 18 - length of bin in years, for working out rates

Filenames: supernova-<opt>-<imf>.<z>.dat

README: Stellar Type Numbers

These files contain the numbers of stars of a given spectral type (where these are selected based on the physical properties as described in E+17, table 3), in a stellar

population at a given age, assuming 10^6 Msun in stars were formed at $t=0$. They give the total number of stars of each type expected at each age.

Each file has 51 rows (one for each age bin) and 21 columns. The first column holds the $\log(\text{age}/\text{years})$ of the population while remaining columns hold the numbers by subtype in two luminosity bins as follows (column - type):

| Luminosity>4.9 | Luminosity<4.9 |
|----------------|----------------|
| 2 - O | 12 - O |
| 3 - Of | 13 - Of |
| 4 - B | 14 - B |
| 5 - A | 15 - A |
| 6 - YSG | 16 - YSG |
| 7 - K | 17 - K |
| 8 - M | 18 - M |
| 9 - WNH | 19 - WNH |
| 10 - WN | 20 - WN |
| 11- WC | 21- WC |

Filenames: numbers-<opt>-<imf>.<z>.dat

README: Yields

These files contain the total yield of hydrogen, helium and metals in supernova ejecta and stellar winds as a function of age, for a population of 10^6 Msun formed at $t=0$.

Each file has 51 rows (one for each age bin) and 9 columns. The first column holds the $\log(\text{age}/\text{years})$ of the population while remaining columns hold:

Stellar Winds:

Col 2 - hydrogen mass output in Msun/yr

Col 3 - helium mass output in Msun/yr

Col 4 - metal mass output in Msun/yr

Col 5 - stellar wind energy output in $\text{Msun m}^2 \text{s}^{-2} / \text{yr}$ (multiply by 2×10^{30} kg and get J/yr).

Supernovae:

Col 6 - supernova energy output in J/yr, assuming 10^{51} ergs per supernova.

Col 7 - hydrogen mass output in Msun/yr

Col 8 - helium mass output in Msun/yr

Col 9 - metals mass output in Msun/yr

Filenames: yields-<opt>-<imf>.<z>.dat

README: Surviving Stellar Masses

These files contain the total mass of the surviving stellar population as a function of age, for a population of 10^6 Msun formed at $t=0$. These do not include the mass in compact remnants.

Each file has 51 rows (one for each age bin) and 2 columns. The first column holds the $\log(\text{age}/\text{years})$ of the population while the second holds the total mass of surviving stars in solar masses.

For the binary files we have included a third, untested, column that includes the mass in stellar remnants, i.e. white dwarfs, neutron stars and black holes. We will add this column to the single star population in future.

Filenames: starmass-<opt>-<imf>.<z>.dat

README: Ionizing Photon Rates

These files contain quantities relating to the ionizing flux from the stellar population as a function of age, for a population of 10^6 Msun formed at $t=0$.

Each file has 51 rows (one for each age bin) and 5 columns. The first column holds the $\log(\text{age}/\text{years})$ of the population while the remainder are as follows:

- 2 - $\log(\text{Nion per second})$ - ionizing photon production rate
- 3 - $\log(L_{\text{H}\alpha} \text{ in ergs/s})$ - Balmer $\text{H}\alpha$ line luminosity, assuming $=\log(\text{Nion/s})-11.87$.
- 4 - $\log(L_{\text{FUV}} \text{ in ergs/s/A})$ - luminosity in the FUV band (mean flux from 1556 to 1576Å).
- 5 - $\log(L_{\text{NUV}} \text{ in ergs/s/A})$ - luminosity in the NUV band (mean flux from 2257 to 2277Å).

Filenames: ionizing-<opt>-<imf>.<z>.dat

README: Colours

These files contain the absolute magnitudes predicted for stellar populations as a function of age, for a population of 10^6 Msun formed at $t=0$, calculated using convolution of the SED with standard filter profiles.

Each file has 51 rows (one for each age bin) and 22 columns. The first column holds the log(age/years) of the population while the remainder are colours (column 2 only) and absolute magnitudes in different filters as follows:

| | | |
|---------|------------|------------|
| 2 - V-I | 10 - K | 18 - f435w |
| 3 - U | 11 - u | 19 - f450w |
| 4 - B | 12 - g | 20 - f555w |
| 5 - V | 13 - r | 21 - f606w |
| 6 - R | 14 - i | 22 - f814w |
| 7 - I | 15 - z | |
| 8 - J | 16 - f300w | |
| 9 - H | 17 - f336w | |

Where U, B, V, R, I are drawn from the standard Johnson-Cousins filter set; J, H and K are the Mauna Kea/2MASS survey profiles; u, g, r, i, z are the SDSS filter set; and F300W, F336W, F450W, F555W, F606W and F814W are the HST/WFPC2 broadband filter set. F435W is in the HST/ACS broadband filter set. All magnitudes are given in the Vega system.

Filenames: colours-<opt>-<imf>.<z>.dat

README: Lick Indices

These files contain quantitative measurements of the standard Lick Index set taken from our spectral energy distributions as described in Stanway & Eldridge 2018. These quantities are presented as linear values (i.e. not as a log) for a population of 10^6 stars, formed at $t=0$, and allowed to evolve over time.

Each file has 51 rows (one for each age bin) and 31 columns. The first column holds the log(age/years) of the population while the remainder are either magnitudes (CN, Mg_1/2, TiO indices) or equivalent widths in Angstroms (all others) in different Lick Indices as follows:

| | | |
|-------------|-------------|----------------|
| 2 - CN_1 | 12 - Mg_1 | 22 - TiO_2 |
| 3 - CN_2 | 13 - Mg_2 | 23 - H_delta_A |
| 4 - Ca4227 | 14 - Mg_b | 24 - H_gamma_A |
| 5 - G4300 | 15 - Fe5270 | 25 - H_delta_F |
| 6 - Fe4383 | 16 - Fe5335 | 26 - H_gamma_F |
| 7 - Ca4455 | 17 - Fe5406 | 27 - Ca8498 |
| 8 - Fe4531 | 18 - Fe5709 | 28 - Ca8542 |
| 9 - Fe4668 | 19 - Fe5782 | 29 - Ca8662 |
| 10 - H_beta | 20 - Na_D | 30 - D4000 |
| 11 - Fe5015 | 21 - TiO_1 | |

Where for the indices in columns 2-26 we use the definition of Worthey & Ottaviani (1997), for columns 27-29 we use those of Du, Luo & Zhao (2012), and D4000 is defined as the ratio of the mean flux in the range 3850-3950 Å to that in the range 4000-4100 Å.

Filenames: lick-<opt>-<imf>.<z>.dat (data format: '(30(e12.4))')

README: Mass-to-Light Ratios

These files contain quantitative measurements of their mass-to-light ratios derived from our models as a function of age. These quantities are presented as linear values (i.e. not as a log) for a population of 10^6 stars, formed at $t=0$, and allowed to evolve over time.

Each file has 51 rows (one for each age bin) and 3 columns. The first column holds the $\log(\text{age}/\text{years})$ of the population. The second column holds the K-band mass-to-light ratio and the third column the V-band mass-to-light ratio. These are given in Solar units (i.e. as multiples of $M_{\text{sun}}/L_{\text{sun}}$), using the Vega-calibrated V and K band data from the 'colours' files and the total mass of remaining stars (not including stellar remnants) from the 'starmass' files in the distribution.

Filenames: mlratio-<opt>-<imf>.<z>.dat (data format: '(3(e12.4))')

README: Hertzsprung-Russell diagram isocontours

These files contain information on theoretical Hertzsprung-Russell diagram isocontours in luminosity, temperature, surface gravity and gravity weighted flux (T^4/g , hereafter TG or L/M) for a population of 10^6 stars, formed at $t=0$, and allowed to evolve over time.

Note: These are large files (~70MB each).

Each file contains a series of 100 row x 100 column grids, ordered by time and hydrogen abundance. Each grid value contains the probability of the grid point being occupied by stars at that time.

The first grid (i.e. the first 100 rows) represents a probability map in $\log T$ (rows) vs $\log L$ (columns) at $\log(\text{age})=6.0$ years for stars with a surface hydrogen abundance $X > 0.4$.

The next fifty grids (i.e rows 101 to 5100) each repeat this while incrementing the age by $\log(\text{age})=0.1$ per grid

Grids 52-102 (rows 5101-10200) are in log T vs log L, incrementing through the 51 age bins, but for stars with a surface hydrogen abundance $0.4 > X > 1e-3$

Grids 103-153 (rows 10201-15300) are in log T vs log L, incrementing through the 51 age bins, but for stars with a surface hydrogen abundance $X < 1e-3$

This sequence is then repeated for grids of probability density in log T (rows) vs log G (columns) - grids 154-306.

And the sequence is repeated again for log T (rows) vs log TG (columns) - grids 307-459

I.e.:

| Grid (n) | Row Parameter | Column Parameter | Hydrogen Abundance | i | Log Age |
|----------|---------------|------------------|--------------------|---------|---------------------|
| 1-51 | Log T | Log L | $X > 0.4$ | n - 1 | $6.0 + 0.1 \cdot i$ |
| 52-102 | Log T | Log L | $0.4 > X > 1e-3$ | n - 52 | $6.0 + 0.1 \cdot i$ |
| 103-153 | Log T | Log L | $X < 1e-3$ | n - 103 | $6.0 + 0.1 \cdot i$ |
| 154-204 | Log T | Log G | $X > 0.4$ | n - 154 | $6.0 + 0.1 \cdot i$ |
| 205-255 | Log T | Log G | $0.4 > X > 1e-3$ | n - 205 | $6.0 + 0.1 \cdot i$ |
| 256-306 | Log T | Log G | $X < 1e-3$ | n - 256 | $6.0 + 0.1 \cdot i$ |
| 307-357 | Log T | Log TG | $X > 0.4$ | n - 307 | $6.0 + 0.1 \cdot i$ |
| 358-408 | Log T | Log TG | $0.4 > X > 1e-3$ | n - 358 | $6.0 + 0.1 \cdot i$ |
| 409-459 | Log T | Log TG | $X < 1e-3$ | n - 409 | $6.0 + 0.1 \cdot i$ |

For each grid, the row and column parameters are gridded as follows:

| Parameter | Minimum | Maximum | Increment |
|-----------|---------|---------|-----------|
| Log T | 0.1 | 10.0 | 0.1 |
| Log L | -2.9 | 7.0 | 0.1 |
| Log G | -2.9 | 7.0 | 0.1 |
| Log TG | -2.9 | 7.0 | 0.1 |

An example IDL plotting code for these files is provided in the *Auxiliary Software* section below.

Filename: hrs-<opt>-<imf>.<z>.dat

README: Inputs

Input files for the BPASS spectral synthesis code are not expected to be user-readable, and are included in the data release directories for archiving purposes. They are also required to generate colour-magnitude diagrams for the populations, using the code we supply.

Row 1 contains the IMF conversion factor to calculate exact number of systems for 1e6 Msun of stars (which in this version is unity).

Each following row gives file-name, model type, and if required model parameters. See section on *Auxiliary Software* for further details

Filename: input_bpass_<z>_<opt>_<imf>.dat

README: Stellar Models

Also included in the distribution are the outputs of our 1D stellar evolution code. These comprise a large library of >200,000 individual stellar models, both for single stars and incorporating the effects of binary evolution. For binaries, we produce both a primary model and a secondary model (which continues evolution of the binary after death of the first star).

The models are stored in directory BPASSv2.1_stellar_models. Within the data release directory, the single star models can be found in file NEWSINMODS.tar and the binary models in NEWBINMODS.<z>.tar.

Warning: These files are large (~500 MB).

They will unpack into a directory structure below the working directory, which separates primary star models from secondary star models and by metallicity.

Filename: sneplot-<z>-M1-q-logP

where, <z> is the metallicity, M1 is the initial mass of the primary star in solar masses, q is M2/M1 (the initial mass of secondary over the initial mass of primary) and logP is the log of the initial orbital period of the binary in days

Or sneplot_2-<z>-M2-Mr-logP

where, $\langle z \rangle$ is the metallicity, M_2 is the mass of the star that was initially the less massive (treated as the primary star in subsequent evolution), M_r is the mass of the remnant left by death of the initially more massive star, and $\log P$ is log of the binary period after formation of the remnant.

The most useful parameters are:

- columns 1-16, parameters of the primary star
- columns 35-38 parameters of the binary
- columns 47-49 parameters of the companion (if undefined no companion or not visible)
- columns 54-73 total magnitudes for binary
- columns 74-93 magnitudes for companion (if undefined no companion or not visible)

Column Number - Variable

- 1 - Model timestep number
- 2 - Age/yr
- 3 - $\log_{10}(R_1/R_{\text{sun}})$ - radius of star 1
- 4 - $\log_{10}(T_{\text{eff}}/K)$ - effective temperature of star 1
- 5 - $\log_{10}(L_1/L_{\text{sun}})$ - luminosity of star 1
- 6 - Total Mass, M_1/M_{sun} - mass of star 1 (use this value not column 37).
- 7 - (He core mass of star 1)/ M_{sun}
- 8 - (CO core mass of star 1)/ M_{sun}
- 9 - (ONe core mass of star 1)/ M_{sun}
- 10 - Empty column
- 11 - Surface mass fractions for X
- 12 - Surface mass fractions for Y
- 13 - Surface mass fractions for C
- 14 - Surface mass fractions for N
- 15 - Surface mass fractions for O
- 16 - Surface mass fractions for Ne
- 17 - (Mass of Hydrogen in star 1)/ M_{sun}
- 18 - (Mass of Helium in star 1)/ M_{sun}
- 19 - (Mass of Carbon in star 1)/ M_{sun}
- 20 - (Mass of Nitrogen in star 1)/ M_{sun}
- 21 - (Mass of Oxygen in star 1)/ M_{sun}
- 22 - (Mass of Neon in star 1)/ M_{sun}
- 23 - (Mass of Magnesium in star 1)/ M_{sun}
- 24 - (Mass of Silicon in star 1)/ M_{sun}
- 25 - (Mass of Iron in star 1)/ M_{sun}
- 26 - Envelope Binding Energy / Joules
- 27 - Total Star binding energy / Joules
- 28 - $M(\text{Remnant})/M_{\text{sun}}$ for weak-SNe ($1e43J$)
- 29 - $M(\text{Ejecta mass})/M_{\text{sun}}$ for weak-SNe ($1e43J$)
- 30 - $M(\text{Remnant})/M_{\text{sun}}$ for SNe ($1e44J$)

- 31 - M(Ejecta mass)/Msun for SNe (1e44J)
- 32 - M(Remnant)/Msun for super-SNe (1e45J)
- 33 - M(Ejecta mass)/Msun for super-SNe (1e45J)
- 34 - Angular momentum of binary
- 35 - Period of binary in years
- 36 - log(Separation of binary/Rsun)
- 37 - Mass of star 1, M1/Msun - use column 6
- 38 - Mass of star 2, M2/Msun
- 39 - Total mass of binary, MTOTAL/Msun
- 40 - DM1W - wind mass loss rate of star 1 (Msun/(1.989*s))
- 41 - DMW2 - wind mass loss rate of star 2 (Msun/(1.989*s))
- 42 - DM1A - accretion of mass (Msun/(1.989*s))
- 43 - DM2A - accretion of mass (Msun/(1.989*s))
- 44 - DM1R - Roche Lobe Overflow of star 1 (Msun/(1.989*s))
- 45 - DM2R - Roche Lobe Overflow of star 2 (Msun/(1.989*s))
- 46 - DANGJJ - Change of angular momentum
- 47 - DLog10(R2/Rsun) - estimated radius of star 2
- 48 - DLog10(T2/K) - estimated effective temperature of star 2
- 49 - DLog10(L2/Lsun) - estimated luminosity of star 2
- 50 - Roche lobe overflux of star 2
- 51 - modelimf - total IMF probability of stars (assuming Kroupa IMF)
- 52 - mixedimf - IMF probability of rejuvenated stars

Following are for total absolute magnitudes and colours of both stars in binary:

- | | | |
|----------|--------|------------|
| 53 - V-I | 60 - H | 67 - f300w |
| 54 - U | 61 - K | 68 - f336w |
| 55 - B | 62 - u | 69 - f435w |
| 56 - V | 63 - g | 70 - f450w |
| 57 - R | 64 - r | 71 - f555w |
| 58 - I | 65 - i | 72 - f606w |
| 59 - J | 66 - z | 73 - f814w |

Following are for the absolute magnitudes of the secondary star in the binary alone:

- | | | |
|--------|------------|------------|
| 74 - U | 81 - K | 88 - f336w |
| 75 - B | 82 - u | 89 - f435w |
| 76 - V | 83 - g | 90 - f450w |
| 77 - R | 84 - r | 91 - f555w |
| 78 - I | 85 - i | 92 - f606w |
| 79 - J | 86 - z | 93 - f814w |
| 80 - H | 87 - f300w | |

Filters are as described under ‘colours’ above. All magnitudes are in the Vega system.

README: O Star Atmosphere Models

In the directory `WMBasic_OB_atmosphere_models`, we provide access to those stellar atmospheres which are used in BPASS spectral synthesis and not publically available elsewhere (these were initially released with v2.1 and should be referenced to E+17).

Our input grid of WM-Basic atmosphere models, calculated specifically for inclusion in BPASS, are described in E+17. Here we do not provide the rebinned versions included in BPASS but the direct output from WM-Basic. Each file has two columns which are wavelength and flux (the 3rd and 4th columns are for continuum subtractions).

The file names are of the form:

`xx_yyyyZ_zz.zzkK.dat`

Where:

- 1) `xx` = sg (supergiant), dw (dwarf) or hg (high gravity).
- 2) `yyyy` = is the metallicity mass fraction as in the standard BPASS grid.
- 3) `zz.zz` = the effective temperature in kK.

The temperature grid for “dw” and “hg” models (surface gravities of $\log(g) = 4.0$ and 4.5 respectively) is: 50.0, 45.7, 42.6, 40.0, 37.2, 34.6, 32.3, 30.2, 28.1, 26.3, 25.0.

For the “sg” models the gravities and surface temperatures are:

$\log(g) = 3.88, 3.73, 3.67, 3.51, 3.40, 3.29, 3.23, 3.14, 3.08, 2.99, 2.95$.

$T/\text{kK} = 51.4, 45.7, 42.6, 40.0, 37.2, 34.6, 32.3, 30.2, 28.1, 26.3, 25.0$.

.

6 - Post-Processed Data Products

CLOUDY and Nebular gas

BPASS produces stellar continuum emission. We caution that, in astrophysical contexts, this is reprocessed by dust and nebular gas before detection, and that our models should be similarly processed. The main consequences of nebular gas interaction is a reduction in the rest-frame ultraviolet and ionizing photon flux from a stellar population, and its reemission as both a nebular continuum component and strong optical and infrared emission lines. Both nebular and line emission are important for interpretation of observed quantities such as spectral slope and line equivalent widths.

We recommend the use of a radiative transfer code such as [CLOUDY](#) or [MAPPINGS](#) to post-process BPASS SSP models.

We have been wary of providing a processed data set, since there is considerable uncertainty on the physical range of nebular gas parameters in any given environment, and it is important to distinguish between uncertainties in the stellar models and those in their later reprocessing.

In published work (e.g. Stanway et al 2014 and our earlier work on BPASS v1.1) we have used CLOUDY v13.03 and defined a default set of nebular gas parameters as follows:

- gas metallicity and abundance pattern matches stellar metallicity,
- $\log(\text{electron density})=2$,
- covering fraction=1,
- spherical geometry with inner radius=10 pc.

These are broadly consistent with typical HII regions in the local Universe. Users should also consider reasonable dissipation times for nebular gas in young stellar clusters (i.e. up to which ages should the models be reprocessed) and potential impacts of the diffuse interstellar medium. These are use-case specific. An alternative is to fix a gas density and vary the ionization parameter.

In Xiao et al (2018 + submitted) we explore a wider range of nebular gas parameters and their effects on the Baldwin, Philipps & Terlevich (BPT) excitation diagrams, including defining maximal starburst (or photoionization limit) lines for the BPASS v2.1 binary populations as a function of metallicity. Very little in v2.2 will affect the nebular emission that comes from young stellar populations (see page 30).

Note that it is also possible to vary gas phase abundance ratios relative to that in the stellar population, which may be important (and even required in, for example, α -enhanced populations).

While we do not provide a nebular gas processed data set, we can offer advice on your own implementation of CLOUDY (although we don't claim to be experts on radiative transfer or CLOUDY itself), or collaboration on more complex projects.

Getting BPASS into CLOUDY:

CLOUDY can accept input irradiation spectra through use of the “interpolate” command. Using this method, any spectrum (including BPASS SED outputs) can be processed by including the following lines in the CLOUDY input parameter file:

```
interpolate{ nu_0      flux_0}  
continue{nu_1  flux_1}{nu_2  flux_2}{nu_3  flux_3} . . . {nu_10 flux_10}  
  . . .  
  . . .  
continue{nu_n-9 flux_n-9}{nu_n-8 flux_n-8}{nu_n-7 flux_n-7} . . . {nu_n flux_n}
```

where `nu_i` and `flux_i` are frequency/luminosity pairs drawn from the irradiating SED at sufficient resolution to capture the behaviour of the input spectrum. Note that, since the spectrum is normalised by CLOUDY, the bolometric luminosity of the input spectrum must also be provided (with the `luminosity` command).

In the most recent data release of CLOUDY (c17.00), Ferland and collaborators have provided a script for importing BPASS models into Cloudy. We believe that this should work with any version as long as the paths and filenames are correct.

We refer users to CLOUDY documentation (at nublado.org and in the associated Hazy manuals) for full details.

Dust Absorption and Re-emission

In addition to processing by nebular gas, the light from astronomical sources is often processed by dust grains in the circumstellar or interstellar medium. This has three main effects: in the rest-frame optical and ultraviolet flux is lost from the line of sight, reddening the spectrum; in the rest-frame infrared and submillimetre, this flux is reemitted as thermal blackbody emission from dust grains or through excitation of polyaromatic hydrocarbons; in nebular regions, dust can interact with nebular gas and deplete certain elemental species. Dust effects are not implemented in the BPASS stellar population and SED models.

Dealing with dust effects on nebular emission is challenging and should be considered in the context of CLOUDY or other radiative transfer models.

Dust extinction is characterised by a wavelength-dependent dust opacity curve, $k(\lambda)$, such that

$$f_{\text{obs}}(\lambda) = f_{\text{int}}(\lambda)10^{-0.4A_\lambda} \quad \text{and} \quad A_\lambda = k(\lambda)E(B - V) = \frac{k(\lambda)A_V}{R_V}$$

Here, $k(\lambda)$ and R_V define the extinction law (which varies with metallicity and environment), and A_V or $E(B-V)$ determine the strength of the dust extinction.

We recommend that users investigate the appropriate dust extinction prescription for their environment and modify the BPASS data release SSP SEDs by a dust curve as appropriate.

Users working with data at wavelengths >3 microns (rest) will likely also need to consider dust in emission. We recommend the use of an energy-balance prescription which reprocesses the total absorbed energy from the best fit extinction curve as a series of blackbody and PAH emission components (see da Cunha et al 2008). This is the approach taken by the MAGPHYS galaxy SED code.

Note that BPASS does not provide dust-processed models and is not itself an SED-fitting code, but can be incorporated in existing codes. Again, we can discuss implementation with interested users.

Complex Star Formation Histories

Complex or composite (i.e. non-co-eval) stellar populations are not provided as a part of our standard release but can be constructed by assuming a star formation history and combining models of different ages in the correct proportion to reconstruct a mixed-age population.

The simplest case is a population forming stars continuously at a constant rate.

Here the only potential difficulty lies in dealing with logarithmically spaced time intervals in the models since the total number or fraction of stars to be added to the composite spectrum depends on the width of the interval. Stars contributing to the flux, stellar type numbers or rates in the first BPASS time bin (at $\log(\text{age}/\text{years})=6.0$) include all members of the population up to $\log(\text{age})=6.05$ (i.e. $\Delta t_0 = 10^{6.05}$), the second bin includes stars in the range $\log(\text{age})=6.05$ to 6.15 years and so forth (i.e.

$$\Delta t_i = 10^{6.15+0.1i} - 10^{6.05+0.1i} \quad \text{for } i > 0).$$

Thus

$$F(\lambda) = f_0(\lambda) \Delta t_0 + \sum_{i=1}^{\max} f_i(\lambda) \Delta t_i$$

Where $F(\lambda)$ is the flux of the composite population, f_i is the flux of simple stellar population in age bins, i , and the upper limit “max” is the time bin corresponding to the observed age of the composite population after the initial onset of star formation.

For other complex star formation histories, a similar prescription can be adopted, while noting that care must be taken not to confuse the age of a stellar population in a time bin with the ‘age’ of the composite stellar population since the onset of star formation:

$$F(\lambda) = \Psi_0 f_0(\lambda) \Delta t_0 + \sum_{i=1}^{\max} \Psi_i f_i(\lambda) \Delta t_i$$

where Ψ_i is the star formation rate (per year) that was experienced by stars which formed in the population at a time before present (or observation, i.e. $i=\max$) corresponding to the age of stars in bin i .

7 - Recent Key Results and Calibration Tables

For ease of reference, we provide here a few tables and results drawn from recent papers which are likely to be more generally useful. These results assume our default, broken power law IMF with an upper slope of -1.35 and $M_{\text{max}}=300$ Msun.

Please reference the original papers if using these numbers.

Note, some of these have not yet been modified for v2.2.

Z-dependent Star Formation Rate Conversion Factors for $H\alpha$ and FUV

Ref: Eldridge, Stanway et al (2017, E+17, tab 4), Updated to **v2.2** (Stanway & Eldridge 2018). Please use both references for this data table.

Since the ionizing flux arising from a stellar population is strongly metallicity dependent, we derive a set of metallicity-dependent star formation rate conversion factors for two key observables: the $H\alpha$ emission line, and the rest-frame 1500Å luminosity. These are for a population forming stars at a constant rate, and which has been doing so for long enough for the flux to stabilise (typically ~ 300 Myrs)

The table below provides values $\log(\dot{M}/M_{\odot} \text{ yr}^{-1}) = \log(L/\text{erg s}^{-1}) - C(Z)$ $C(Z)$ such that:

| Z | $\log H\alpha$ | | $\log[\nu L_{\nu}(1500)]$ | |
|-----------|----------------|-------|---------------------------|-------|
| | bin | sin | bin | sin |
| 10^{-5} | 41.85 | 41.71 | 43.45 | 43.42 |
| 10^{-4} | 41.80 | 41.68 | 43.45 | 43.42 |
| 0.001 | 41.74 | 41.62 | 43.42 | 43.37 |
| 0.002 | 41.71 | 41.59 | 43.40 | 43.36 |
| 0.003 | 41.69 | 41.57 | 43.39 | 43.34 |
| 0.004 | 41.66 | 41.54 | 43.39 | 43.33 |
| 0.006 | 41.61 | 41.52 | 43.39 | 43.32 |
| 0.008 | 41.58 | 41.49 | 43.37 | 43.31 |
| 0.010 | 41.54 | 41.46 | 43.37 | 43.30 |
| 0.014 | 41.48 | 41.41 | 43.34 | 43.29 |
| 0.020 | 41.42 | 41.34 | 43.32 | 43.27 |
| 0.030 | 41.31 | 41.23 | 43.29 | 43.23 |
| 0.040 | 41.25 | 41.15 | 43.26 | 43.19 |

Maximal relations for BPASS binary starbursts in the BPT diagrams.

Ref: Xiao, Eldridge & Stanway (2018), [v2.1](#)

For each of the three BPT diagrams, and at each metallicity in our model grid, we define a set of metallicity- dependent maximal starburst lines derived using BPASS v2.1 and CLOUDY radiative transfer models described in this paper. These are a set of equations for an upper locus which encloses all possible star formation powered HII regions with $0 < \log(nH) < 3$, $-3.5 < \log(U) < -1.5$ and $6.0 < \log(\text{Age/yr}) < 7.5$, assuming the inclusion of binary star populations. We use the same functional form as Kewley et al (2001):

$$\log([\text{O III}]/\text{H}\beta) = \frac{A_i}{\log(X_i) + B_i} + C_i, \quad (\text{A1})$$

where $X_i = [\text{N II}]/\text{H}\alpha$, $[\text{S II}]/\text{H}\alpha$ or $[\text{O I}]/\text{H}\alpha$, while A , B and C are constants. We also derive a line encompassing all metallicities.

| Z | $X_1 = [\text{N II}]/\text{H}\alpha$ | | | $X_2 = [\text{S II}]/\text{H}\alpha$ | | | $X_3 = [\text{O I}]/\text{H}\alpha$ | | |
|--------------------|--------------------------------------|-------|-------|--------------------------------------|-------|-------|-------------------------------------|-------|-------|
| | A_1 | B_1 | C_1 | A_2 | B_2 | C_2 | A_3 | B_3 | C_3 |
| 1×10^{-5} | 0.74 | 2.31 | -0.72 | 0.92 | -0.91 | -0.64 | 1.04 | 0.01 | -0.62 |
| 1×10^{-4} | 0.78 | 1.27 | 0.26 | 0.72 | -0.77 | 0.26 | 1.00 | 0.03 | 0.32 |
| 0.001 | 0.52 | 0.42 | 0.98 | 0.50 | -0.59 | 1.00 | 0.64 | 0.27 | 1.02 |
| 0.002 | 0.42 | 0.20 | 1.14 | 0.44 | -0.55 | 1.16 | 0.50 | 0.05 | 1.16 |
| 0.003 | 0.32 | 0.13 | 1.18 | 0.44 | -0.51 | 1.26 | 0.54 | -0.15 | 1.28 |
| 0.004 | 0.28 | 0.11 | 1.12 | 0.54 | -0.41 | 1.30 | 0.40 | 0.03 | 1.18 |
| 0.006 | 0.26 | 0.00 | 1.22 | 0.40 | -0.35 | 1.32 | 0.36 | -0.19 | 1.26 |
| 0.008 | 0.26 | -0.08 | 1.26 | 0.34 | -0.23 | 1.32 | 0.38 | -0.23 | 1.32 |
| 0.010 | 0.28 | -0.15 | 1.28 | 0.36 | -0.17 | 1.36 | 0.32 | -0.19 | 1.30 |
| 0.014 | 0.28 | -0.24 | 1.36 | 0.28 | -0.05 | 1.38 | 0.18 | -0.19 | 1.28 |
| 0.020 | 0.18 | -0.13 | 1.28 | 0.22 | 0.15 | 1.32 | 0.14 | -0.05 | 1.24 |
| 0.030 | 0.18 | -0.13 | 1.24 | 0.20 | -0.63 | 1.26 | 0.18 | 0.09 | 1.24 |
| 0.040 | 0.32 | -0.18 | 1.30 | 0.24 | -0.35 | 1.28 | 0.30 | 0.25 | 1.30 |
| All | 0.28 | -0.26 | 1.36 | 0.82 | 0.70 | 1.61 | 0.19 | 0.80 | 1.31 |

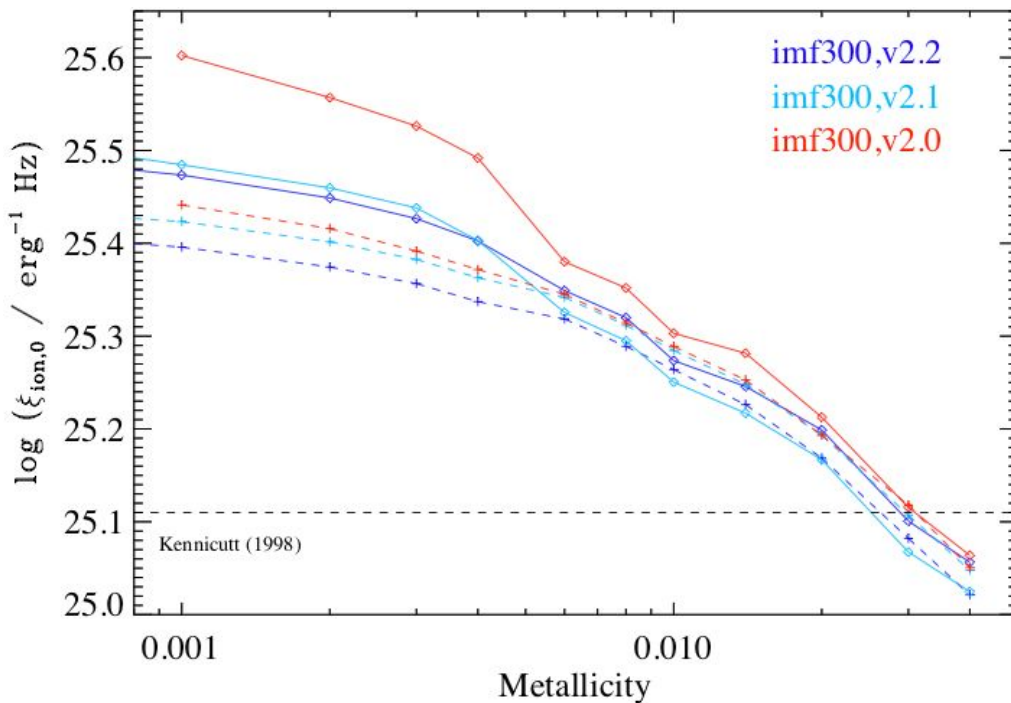
Rest-Ultraviolet Properties of Ongoing Starbursts (N_{ion} , L_{1500} , ξ_{ion})

Ref: Stanway, Eldridge & Becker (2016), updated to use the **v2.2** models of Stanway & Eldridge 2018. Please use both references for this data table.

Here we update the data table of Stanway et al (2016) to reflect values for our newest v2.2 models, given our default IMF. Please see the original paper and E+17 for detailed definitions of $\xi_{\text{ion},0}$ (the ionizing photon production efficiency, assuming no escape fraction).

| Z | $\log N_{\text{ion}}$ | | $\log[L_{1500}/L_{\odot}]$ | | $\log[\xi_{\text{ion},0}]$ | |
|-----------|-----------------------|-------|----------------------------|------|----------------------------|-------|
| | bin | sin | bin | sin | bin | sin |
| 10^{-5} | 53.71 | 53.58 | 6.65 | 6.61 | 25.60 | 25.51 |
| 10^{-4} | 53.67 | 53.55 | 6.66 | 6.63 | 25.55 | 25.45 |
| 0.001 | 53.60 | 53.49 | 6.65 | 6.62 | 25.49 | 25.41 |
| 0.002 | 53.58 | 53.46 | 6.65 | 6.61 | 25.46 | 25.39 |
| 0.003 | 53.55 | 53.44 | 6.65 | 6.61 | 25.44 | 25.37 |
| 0.004 | 53.53 | 53.41 | 6.65 | 6.60 | 25.42 | 25.35 |
| 0.006 | 53.48 | 53.39 | 6.66 | 6.60 | 25.36 | 25.33 |
| 0.008 | 53.44 | 53.35 | 6.65 | 6.59 | 25.33 | 25.30 |
| 0.010 | 53.40 | 53.32 | 6.65 | 6.59 | 25.28 | 25.27 |
| 0.014 | 53.35 | 53.28 | 6.63 | 6.58 | 25.26 | 25.24 |
| 0.020 | 53.29 | 53.21 | 6.62 | 6.57 | 25.21 | 25.18 |
| 0.030 | 53.17 | 53.10 | 6.61 | 6.55 | 25.11 | 25.09 |
| 0.040 | 53.11 | 53.02 | 6.59 | 6.53 | 25.06 | 25.03 |

Observable and inferred parameters from our model $10^6 M_{\odot}$ stellar populations for a system undergoing star formation at a constant rate of $1 M_{\odot} \text{ yr}^{-1}$, observed at an age of 100 Myr after the onset of star formation at which point the fluxes have stabilised. Rest frame 1500\AA luminosities are given in multiples of L_{\odot} per angstrom and photon rates in s^{-1} . $\xi_{\text{ion},0}$ is the ionizing photon production efficiency.



Z-dependent SN Rates for Constant SFR

Ref: [v2.2](#) models of Stanway & Eldridge 2018.

In the data release we provide tables of SN numbers by subtype for simple stellar populations. The table below provides the total rate per year of core-collapse supernovae (i.e. types Ib+Ic+II-P+II-other) and GRBs (QHE pathway only, see v2.1 paper) for our standard population, assuming constant star formation.

| Z | log(CCSN Rate) | | Log(GRB Rate) | |
|-----------|----------------|--------|---------------|-----|
| | bin | sin | bin | sin |
| 10^{-5} | -1.972 | -1.922 | -3.641 | — |
| 10^{-4} | -1.963 | -1.908 | -3.862 | — |
| 0.001 | -1.950 | -1.834 | -3.527 | — |
| 0.002 | -1.964 | -1.834 | -3.601 | — |
| 0.003 | -1.985 | -1.861 | -3.685 | — |
| 0.004 | -1.988 | -1.852 | -3.810 | — |
| 0.006 | -2.036 | -1.861 | — | — |
| 0.008 | -2.032 | -1.891 | — | — |
| 0.010 | -2.033 | -1.940 | — | — |
| 0.014 | -2.046 | -1.953 | — | — |
| 0.020 | -2.071 | -1.962 | — | — |
| 0.030 | -2.151 | -2.076 | — | — |
| 0.040 | -2.128 | -2.083 | — | — |

The rates of core-collapse supernovae (CCSNe) and gamma-ray bursts (GRBs) per year in our canonical models, assuming constant star formation at the rate of $1 \text{ M}_{\odot} \text{ yr}^{-1}$, and that the rates have had sufficient time to stabilise (i.e. SFR has been constant for $>100 \text{ Myr}$. This GRB rate is isotropic (i.e. not corrected for beaming angle) and assumes only pathways involving spin up by mass accretion and rotationally-mixed, chemically homogenous evolution. Other pathways may not be accounted for. Where no number is provided, these events are sufficiently rare not to be represented in our standard synthesis models.

8 - Auxilliary Software

In the directory “BPASSv2.1_example_plot_routines” we provide a number of plotting scripts to provide examples of reading in and manipulating our data files. These are in the IDL scripting languages. Python users looking for guidance and puzzled by the codes may find online “Numpy for IDL users” resources helpful.

Note, these have not yet been modified for v2.2. Most will work smoothly as long as the filenames and paths are updated.

CMD plotting code - plot1cmdmake.pro and plot1cmdplot.pro

The input_bpass_* files are required by the CMD calculation code. The information taken from them is as follows:

Row (a) - Filename of model to load

Row (b) - Model imf probability and model type

Model type, 0=merger model, 1=normal primary, 2=normal secondary, 3=single star secondary model, 4=binary QHE secondary model

if(modeltype is 2 or greater) then read in more lines:

Row (c) - Mixed imf and mixed age (number of models that are rejuvenated to the mixed age)

For modeltype 4 also read in:

Row (d) - initialblackhole and initial period (initial binary parameters for QHE system to follow widening of orbit due to mass loss from stellar winds alone, QHE stars get smaller during main sequence so shouldn't interact otherwise).

The supplied IDL code reads these input files, then calls on the appropriate stellar models to determine the colours and magnitudes of each star in the population, before weighting these appropriately to create a colour-magnitude diagram.

The file “plot1cmdmake.pro” performs the above binning and outputs the results into IDL save files, this is advisable as it takes time to go through a large number of stellar models. The code will need to be modified so that it points to the correct location for the binary models. It should put to the directory where it can find the “NEWBINMODS” and “NEWSINMODS” directories created once the available stellar model tar files are unpacked.

The file “plot1cmdplot.pro” then creates plots from these save files and should just need to be run from the same directory as the “make” code.

We note with this code it is possible to modify to work out any colour or filter as listed in the above readme descriptions. If advice is required please feel free to contact the BPASS team.

Example plotting codes

We also supply the following IDL codes to plot various output files and properties in the main data release:

- `plot1colours.pro`
- `plot1starmass.pro`
- `plot1numbers.pro`
- `plot1supernova.pro`
- `plot1yields.pro`
- `plot1ionizing.pro`
- `plot1hr.pro`
- `plot1spectra.pro`

Each file loads in *all* the output files over metallicities and IMFs, assuming it is in a directory level equivalent to all the output from the downloadable tar files (this may take a while!).

Each file will then plot each variable, e.g. $M(B)$ colour, for each IMF on the same panel, allowing a direct comparison. They are simple and can be modified to only plot one IMF by just changing the “for” loop limits.

9 - Areas under Development

We are aware of many areas in which BPASS models can be improved.

Key areas on which we are actively working include the following:

- Abundances (varying the input elemental abundance ratios)
- Rotation (improved implementation of rotational mixing and other effects of spin up due to angular momentum transfer)
- Spectral resolution (primarily dependent on improved atmosphere models becoming available at all metallicities)
- Accretion luminosities (derived based on mass transfer and an assumed SED for accreted material onto WD, NS or BHs)
- Complex star formation histories (combining SSPs to model mature galaxies more effectively)
- Gravitational Wave Chirp Event rates and double-degenerate Type Ia supernovae.

While suggestions for future developments are always welcome, we cannot promise a rapid response to specific requests!

10 - The BPASS Team

J.J. Eldridge is a senior lecturer at the University in Auckland in New Zealand. They work primarily on theoretical models of stellar evolution and stellar population synthesis. Email: j.eldridge@auckland.ac.nz

E.R. Stanway is an associate professor at the University of Warwick in the United Kingdom. Her work focuses on the stellar populations of star forming galaxies and transient hosts, and their evolution over cosmic time. Email: e.r.stanway@warwick.ac.uk

L. Xiao is a postdoctoral research associate at the Department of Astronomy, University of Science and Technology of China, having recently completed a PhD at the University of Auckland. Her research centres on the nebular emission from young stellar populations.

L.A.S. McClelland is a PhD candidate at the University of Auckland. His research involves improved modelling of helium giants.

J.C. Bray has recently completed a PhD at the University of Auckland. His research focuses on an improved prescription for the distribution of kick velocities for neutron star and black hole production.

S.M.L. Greis has recently completed a PhD at the University of Warwick. Her research focused on the stellar populations in local analogue galaxies to the distant Universe. She is now leaving astronomy to work as a Data Scientist.

This manual was generated by Elizabeth Stanway and JJ Eldridge. Suggestions for improvement are always welcome.

Thanks

This work would not have been possible without use of the NeSI Pan Cluster, part of the NeSI high-performance computing facilities. New Zealand's national facilities are provided by the NZ eScience Infrastructure and funded jointly by NeSI's collaborator institutions and through the Ministry of Business, Innovation & Employment's Research Infrastructure programme. URL: <https://www.nesi.org.nz>.

We also made use of the University of Warwick's Scientific Computing Research Technology Platform (SCRTP).

JJE acknowledges travel funding and support from the University of Auckland.

ERS acknowledges travel funding and support from the University of Warwick.

We acknowledge very many useful and interesting discussions with BPASS users and collaborators past, present and future, too numerous to name.

We note that BPASS development began when the PIs were post-doctoral researchers and we thank our previous employers (University of Bristol, University of Cambridge, Queen's University Belfast and the Institute d'Astrophysique de Paris) for supporting our use of time on this work.

BPASS is human-resource limited and further iterations will be dependent on the PIs securing research funding in future years.